Superoxide anions regulate TORC1 and its ability to bind Fpr1:rapamycin complex

Taavi K. Neklesa and Ronald W. Davis*

Department of Biochemistry, Stanford University School of Medicine, Stanford, CA 94305

Contributed by Ronald W. Davis, August 6, 2008 (sent for review May 5, 2008)

The small natural product rapamycin, when bound to FKBP12, is a potent inhibitor of an evolutionarily conserved Target of Rapamycin Complex 1 (TORC1), which plays a central role in mediating cellular response to nutrient availability. Given the prominent role of TORC1 in cell growth and proliferation, clinical trials have explored the possibility of using rapamycin as an anticancer agent. Unfortunately, the percentage of patients responding favorably has been low, intensifying the need to find biomarkers able to predict rapamycin sensitivity or resistance. In this study, we elucidate the molecular mechanism underlying partial rapamycin resistance in yeast. Using the yeast deletion collection, we identified 15 deletion strains leading to partial rapamycin resistance. Among these were Cu/Zn-superoxide dismutase Sod1, copper transporter Ctr1, and copper chaperone Lys7, suggesting a role for oxidative stress in rapamycin resistance. Further analysis revealed that all 15 strains exhibit elevated levels of superoxide anions, and we show that elevated levels of reactive oxygen species specifically modify TORC1 such that it is no longer able to fully bind FKBP12:rapamycin. Therefore, elevated oxidative stress modifies TORC1 and prevents its binding to the FKBP12:rapamycin complex, ultimately leading to rapamycin resistance. These results warrant an examination into whether similar reasons explain rapamycin resistance observed in various clinical samples.

Gln3 | rapamycin resistance | ROS | Sod1

In recent years, rapamycin and its analogs have garnered a great deal of interest as chemotherapeutics. Rapamycin first binds a small intracellular protein, FKBP12, forming an FKBP12:rapamycin complex that then tightly binds to TOR kinase. TOR coordinates cell growth and proliferation in response to nutrients present in the microenvironment (1, 2). Purification of TOR from yeast and human cells revealed that TOR can exist in at least two multiprotein complexes. In one, termed TORC1, TOR is associated with raptor; and in the other, termed TORC2, TOR is associated with rictor (3, 4). Interestingly, unlike TORC1, TORC2 cannot be directly inhibited by rapamycin (5, 6). TORC1 and TORC2 appear to have differing substrate specificities both in yeast and human cells (3, 7). TORC1 has been shown to control a diverse set of effector pathways, such as ribosome biogenesis, nutrient catabolism and transport, stress response, and autophagy (1).

In most cell types, rapamycin reaches its full effect at low nanomolar concentrations, as measured by the phosphorylation state of mammalian TORC1 substrate pThr389 S6K1 (8, 9). However, rapamycin sensitivity can vary widely between different tissues and cell lines (10, 11). For example, among the National Cancer Institute human tumor cell line panel of 60 cell lines, only 13 have a half-maximal inhibitory concentration (IC_{50}) below 20 nM, whereas 14 have an IC_{50} higher than 1,000 nM (see http://dtp.nci.nih.gov). Correspondingly, the results from early clinical studies using rapamycins as anticancer agents have been mixed. Among 21 patients, the rapamycin analog CCI-779 showed partial activity in only one patient against metastatic melanoma (12). In treating recurrent glioblastoma, only 7.8% of patients showed progression-free survival at 6 months (13), and CCI-779 had a response rate of 38% in patients with mantle cell lymphoma (14). A recent large-scale phase 3 study with the rapamycin analog Temsirolimus for the treatment of renal cell carcinoma (RCC) showed an objective response rate of 8.6% and median overall survival of 10.9 months (15). These results were an improvement over the efficacy of IFN alpha, which was the main treatment option for RCC, and led to the approval of Temsirolimus for treatment of RCC by the Food and Drug Administration in 2007. Recently, clinical trials have used the phosphorylation state of pSer 240/244 on S6 as a marker to determine the efficacy of rapamycin (16–18). However, care must be exercised with interpreting these data, as S6K1 (a kinase for pSer240/244 S6 and a direct substrate of TORC1) phosphorylation is much more sensitive to rapamycin treatment than cell proliferation (8). Similarly, even at high concentrations of rapamycin, yeast cells maintain their proliferative ability, albeit slow, whereas the TORC1 activity toward its substrate Sch9 is abolished (7). Further, inactivation of TORC1 by rapamycin treatment or deletion of Kog1 (yeast raptor) is not congruent. Kog1, which is an integral TORC1 component not shared with TORC2, is an essential gene, whereas treatment of cells with rapamycin only leads to a cytostatic decrease in proliferation. This suggests that either rapamycin is not able to completely abolish TORC1 activity or that raptor has an essential function beyond TORC1. Clearly, our understanding of TORC1 inhibition by rapamycin is incomplete, especially the relationship between TORC1 kinase activity and cell proliferation. Uncovering these details would enable clinicians to predict *a priori* whether a particular tumor is sensitive or resistant to rapamycin, and therefore help to define the pool of patients most likely to benefit from a rapamycin treatment regimen.

As the TORC1 complex and its role in mediating the signal about nutrient availability are conserved from yeast to humans, we sought to characterize the molecular mechanism of partial rapamycin resistance in yeast. Here, we demonstrate that elevated levels of superoxide anions modify yeast TORC1 such that it is no longer fully able to be inhibited by the FKBP12:rapamycin complex, and the cells with elevated oxidative stress are therefore partially rapamycin resistant.

Results

Identification of Rapamycin-Resistant and Sensitive Deletion Strains. Rapamycin treatment leads to inhibition of cell growth and proliferation. To find genetic determinants that might explain the wide range of rapamycin sensitivity, we performed a genetic screen in yeast for genes that affect the degree of rapamycin toxicity using the yeast deletion collection (19). We grew pooled deletion strains in the presence of 7.5 ng/ml (6.9 nM) of rapamycin for 36 h and collected time points at every 12 h. As expected, the strain missing the rapamycin receptor FKBP12 (encoded by *FPR1* in yeast) exhibited strong rapamycin resistance (Fig. 1*A*). In total, we identified 16 rapamycin-resistant deletion strains, including the fpr1Δ strain (Table 1). By and large, most of these deletion strains have been identified in previous genome-wide screens (20, 21), yet the

Author contributions: T.K.N. and R.W.D. designed research; T.K.N. performed research; R.W.D. contributed new reagents/analytic tools; T.K.N. analyzed data; and T.K.N. wrote the paper.

The authors declare no conflict of interest.

*To whom correspondence should be addressed. E-mail: dbowe@stanford.edu.

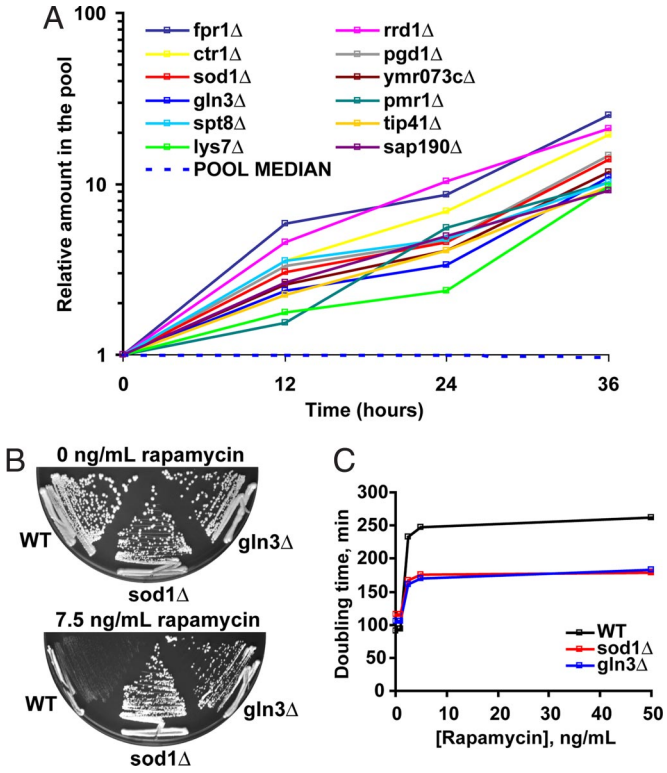

Fig. 1. Identification of rapamycin-resistant strains. (*A*) All nonessential diploid yeast deletion strains were grown pooled in the presence of 7.5 ng/ml rapamycin for 36 h. For each time point, genomic DNA was isolated, and the DNA barcodes were amplified by PCR. The relative level of each deletion strain in the pool was inferred by hybridizing the barcodes to a complementary oligonucleotide array. Shown are 12 representative deletion strains whose relative level in the pool increases. (*B*) Yeast lacking Sod1 or Gln3 are rapamycin-resistant compared with WT strain. Indicated haploid strains were plated on YPD plates containing 0 or 7.5 ng/ml rapamycin for 2 or 4 days, respectively. (*C*) Doubling time for indicated haploid strains in the presence of increasing concentrations of rapamycin was determined by optical density measurements. Representative data are shown.

nature of this resistance has remained unknown. There were two clear categories of resistant strains. One is composed of strains missing components responsible for activity of transcription factor Gln3, which promotes transcription of nitrogen catabolite repression genes upon nitrogen starvation or rapamycin treatment. The second category is composed of strains responsible for detoxifying superoxide anions: Cu/Zn-superoxide dismutase Sod1 and its auxiliary proteins copper transporter Ctr1 and copper chaperone Lys7 (22). Besides resistance conferring deletions, we also identified deletion strains that exhibit rapamycin hypersensitivity. In particular, a set of genes encoding proteins necessary for *de novo* biosynthesis of serine, threonine, and glycine exhibited strong rapamycin sensitivity (Table 1).

To establish a molecular understanding of rapamycin resistance, we decided to further characterize gln3Δ and sod1Δ strains with respect to rapamycin treatment. Both gln3Δ and sod1Δ cells are partially rapamycin resistant, with a maximal doubling time of about 180 min compared with that of about 260 min for WT cells (Fig. 1 *B* and *C*). The observation that the doubling time of the two mutant strains reaches a plateau and remains lower than the doubling time of WT cells at increasing concentrations of rapamycin suggests that resistance in gln3Δ and sod1Δ strains is not a result of differences in the transport or metabolism of rapamycin.

Characterization of the Rapamycin Response in sod1Δ and gln3Δ Strains. To obtain an understanding of how rapamycin resistance is achieved in gln3Δ and sod1Δ strains, we examined whether some or

Table 1. List of rapamycin-resistant deletion strains and a partial list of rapamycin-sensitive deletion strains

Strains	Gene	Function
Rapamycin-resistant deletion strains		
Gln3 activation pathway	*GLN3*	Transcription factor
	TIP41	Regulator of Gln3
	SAP190	Protein phosphatase activator
	RRD1	Protein phosphatase 2A subunit
	PPM1	Protein phosphatase activator
	NPR1	Protein kinase
Superoxide anion detoxification-related	*SOD1*	Cu,Zn superoxide dismutase
	LYS7	Copper chaperone for Sod1
	CTR1	Copper transporter
Transcription machinery	*PGD1*	RNA polymerase II holoenzyme subunit
	SPT8	Part of histone acetyltransferase complex
	PHO23	Histone deacetylase 1
	DEP1	Transcriptional modulator
Other	*PMR1*	Ca^{2+} and Mn^{2+} transport
	YMR073C	Nitrate reductase homolog
Rapamycin-sensitive deletion strains (partial list)		
Serine, threonine, and glycine biosynthesis	*THR1*	Homoserine kinase
	THR4	Threonine synthase
	SER1	Phosphoserine transaminase
	SER2	Phosphoserine phosphatase
	HOM2	Aspartic beta semi-aldehyde dehydrogenase
	HOM3	Aspartate kinase
	HOM6	Homoserine dehydrogenase
	SHM2	Serine hydroxymethyltransferase

all of the TORC1 effector pathways are repressed in response to rapamycin treatment. First, we examined the gene expression profile elicited by rapamycin in gln3Δ and sod1Δ strains. Rapamycin treatment leads to a robust activation of nitrogen catabolism-related genes and to inactivation of genes responsible for ribosome biogenesis (23). We reasoned that if rapamycin resistance in the gln3Δ and sod1Δ strains is caused by universal dampening of rapamycin response, then one would expect the activation of nitrogen catabolism enzymes and inactivation of ribosomal genes to be less robust in gln3Δ and sod1Δ strains. Indeed, we find that genes induced by rapamycin are induced less in gln3Δ and sod1Δ strains and, conversely, genes that are repressed by rapamycin are repressed less in those two strains (Fig. 2 *A* and *B*). We have verified these findings by repeating the microarray experiment and by performing RT-PCR on individual transcripts (data not shown). Therefore, rapamycin appears to be uniformly less potent in activating or repressing transcriptional response in gln3Δ and sod1Δ strains.

Second, we examined the effect of rapamycin on inactivating amino acid transporters in gln3Δ and sod1Δ strains. As noted in Table 1, several of the rapamycin-hypersensitive strains lack Thr, Leu, and Gly biosynthesis genes. Therefore, rapamycin appears to be inactivating transporters responsible for importing these amino acids into cells. We decided to determine whether this inactivation is dampened in gln3Δ and sod1Δ cells. When WT cells are treated with rapamycin, their uptake of radiolabeled Thr is almost completely abolished (Fig. 2*C*). However, the same treatment leads to only a moderate decrease in Thr uptake in gln3Δ and sod1Δ strains. To functionally verify these data, we tested whether deletion of *GLN3* or *SOD1* from a strain that is missing one of the amino acid biosynthesis genes shown in Table 1 would rescue the rapamycin hypersensitivity phenotype. Deletion of *HOM2*, which catalyzes the

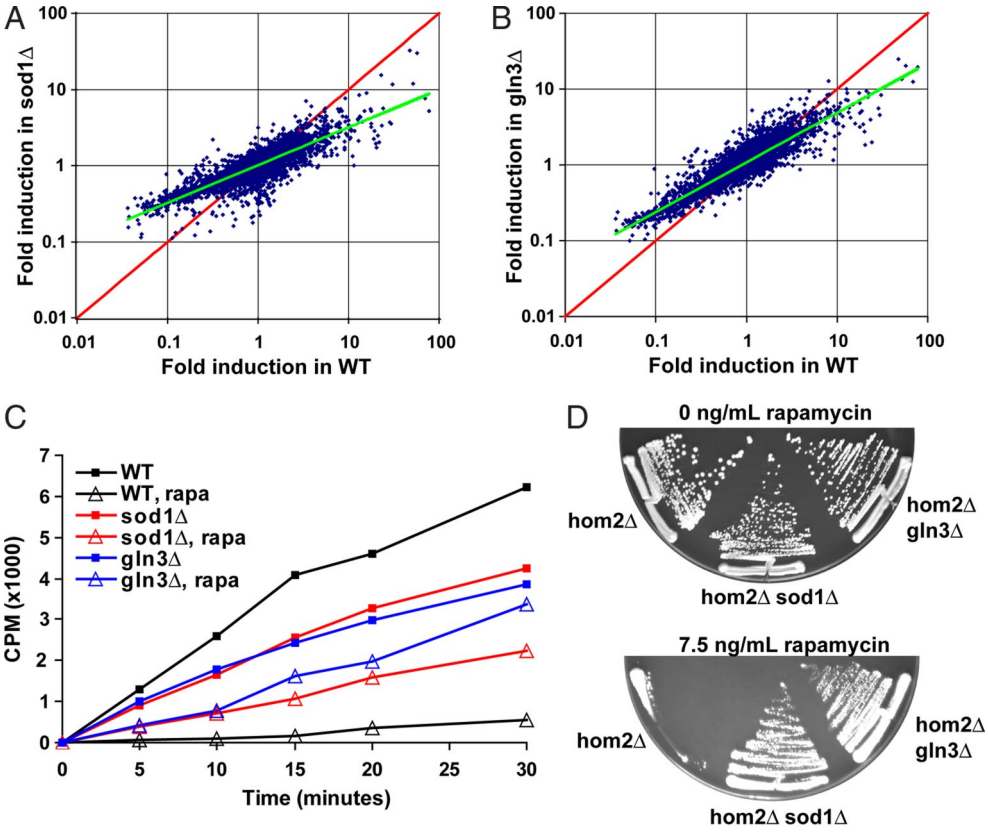

Fig. 2. Deletion of Sod1 or Gln3 lessens the effect of rapamycin. (*A*) Rapamycin elicits a less robust gene expression response in sod1Δ and gln3Δ cells. Genome-wide microarray experiment was carried out on diploid WT and sod1Δ cells treated with either 0 or 20 ng/ml rapamycin for 30 min. The induction ratio for each transcript was calculated by dividing the transcript level in rapamycin-treated culture over the transcript level in non–rapamycin-treated culture. For WT cells, this ratio is plotted for each gene on the *x* axis, and the corresponding ratio for sod1Δ cells is plotted on the *y* axis. No difference was observed between two non–rapamycin-treated samples (data not shown). (*B*) Similar analysis as in A, but gln3Δ induction ratio is plotted on the *y* axis. (*C*) Rapamycin fails to fully inactivate threonine amino acid transporter in sod1Δ and gln3Δ cells. WT, sod1Δ, and gln3Δ diploid cells were grown in the presence (7.5 ng/ml) or absence of rapamycin, and their ability to import [^{3}H]Thr was measured by determining the radioactivity retained by washed cells. Time 0 indicates addition of [^{3}H]Thr into medium. (*D*) Rapamycin hypersensitivity of hom2Δ cells can be rescued by deleting *SOD1* or *GLN3*. Cells with indicated genotypes were plated on YPD plates containing 0 or 7.5 ng/ml rapamycin for 2 or 4 days, respectively.

second step in threonine biosynthesis, renders cells completely unable to grow in the presence of rapamycin, whereas hom2Δ gln3Δ and hom2Δ sod1Δ cells grow normally (Fig. 2*D*). Therefore, we conclude that rapamycin fails to fully inactivate Thr import activity in gln3Δ and sod1Δ strains. These results suggest that rapamycin is universally less toxic to gln3Δ and sod1Δ cells than to WT cells.

Fpr1:Rapamycin Complex Binds TOR Kinases More Weakly in Resistant Strains. The results from the previous section suggest when rapamycin-resistant gln3Δ and sod1Δ cells are treated with rapamycin, they respond to the drug, but the magnitude of the response appears diminished. To account for this observation, we tested whether Fpr1:rapamycin complex is fully able to bind to TOR kinase. To test this, we immunoprecipitated genomically epitope-tagged Fpr1 from WT, gln3Δ, and sod1Δ cells treated with rapamycin, then separated the immunoprecipitates electrophoretically by SDS/PAGE and determined the amount of TOR kinase bound to Fpr1 immunoprecipitates. Yeast, through an ancient genome duplication event, has two TOR kinases: Tor1 and Tor2. We first determined the total amount of TOR immunoprecipitated by Fpr1 by staining the gel with Sypro Ruby stain. Since Tor1 and Tor2 are large ≈280-kDa proteins with exactly the same molecular weight, this stain will detect the sum total of Tor1 and Tor2 kinase bound to Fpr1. As expected, in the absence of rapamycin, no binding takes place, whereas the inclusion of rapamycin in the media leads to an association of Fpr1 and TOR kinases (Fig. 3*A*, *Top*). Consistent with the incomplete binding model, this association is weakened in the gln3Δ and sod1Δ strains, where Fpr1 and TOR kinases associate ≈60% as much as in the WT strain (Fig. 3*B*). When the immunoprecipitates are probed with Tor1 and Tor2 antibodies, we find that in both resistant strains Fpr1 binds to Tor1 and Tor2 at about 70% and 20%, respectively, as much as in the WT cells (Fig. 3*A*, *Second* and *Third*). Interestingly, both sod1Δ and gln3Δ cells exhibit remarkably similar binding capacities between the Fpr1:rapamycin complex and TOR kinases. In the analysis, we also determined that in tor1Δ cells there is an increase in binding between Fpr1 and Tor2 kinase. This finding is consistent with previous observations that the tor1Δ strain is rapamycin hypersensitive (24).

These data clearly demonstrate that in sod1Δ and gln3Δ strains, the Fpr1:rapamycin complex is somehow prevented from binding to the TOR kinases and, presumably, this finding explains why these strains are rapamycin resistant.

All Rapamycin-Resistant Strains Have Elevated Levels of Superoxide Anions. What prevents the Fpr1:rapamycin complex from binding to TOR kinases in rapamycin-resistant strains? The finding that the absence of Cu,Zn-superoxide dismutase Sod1, copper chaperone Lys7, and copper transporter Ctr1 renders cells rapamycin resistant suggests that the elevated levels of superoxide anions might somehow prevent the Fpr1:rapamycin complex from inhibiting TOR kinases. Since the gln3Δ strain exhibits a similar inability to form a Fpr1:rapamycin:TOR complex, we speculated that gln3Δ cells might also possess elevated levels of superoxide anions, which confer rapamycin resistance by the same mechanism as in the sod1Δ cells. Gln3 is responsible for transcription of glutamate dehydrogenase and glutamine synthetase, enzymes necessary for converting a trichloroacetic acid (TCA) cycle intermediate α-ketoglutarate to glutamate and glutamine (25). Possibly, the absence of Gln3 would increase the flux through the TCA cycle by abolishing the α-ketoglutarate→glutamate→glutamine shunt pathway, thereby increasing the amount of NADH and $FADH_2$ electron donors produced and delivered to the electron transport chain. When we measured the oxidative stress level with a superoxide anion-sensitive probe, dihydroethidium (26), we found that, indeed, both sod1Δ and gln3Δ cells exhibit elevated levels of superoxide anions (Fig. 4*A*). Furthermore, we found that all 15 rapamycin-resistant strains exhibit elevated levels of superoxide anions (Fig. 4*B*), suggesting that these strains all share a common mechanism of achieving rapamycin resistance.

The inclusion of compounds leading to oxidative stress in the

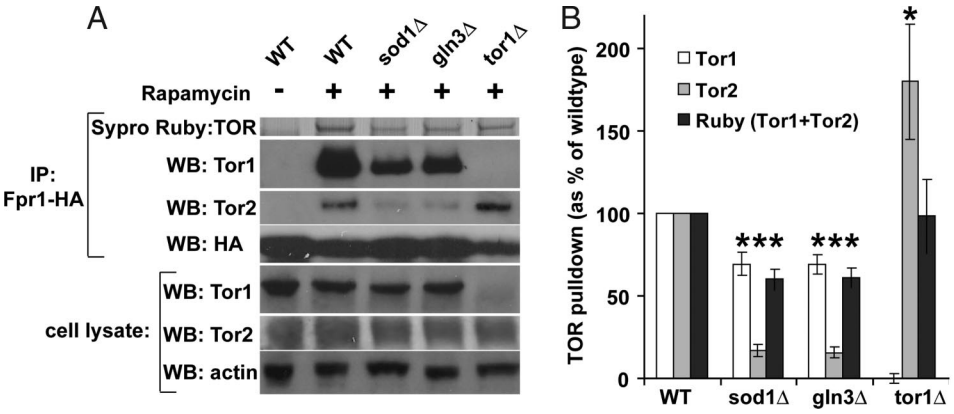

Fig. 3. Fpr1:rapamycin complex can only partially bind to TOR kinases in sod1Δ and gln3Δ strains. (*A*) Indicated deletion strains expressing genomic Fpr1-HA were grown in the absence (only WT) or presence of 5 ng/ml rapamycin for 2 h. Anti-HA immunoprecipitates were separated on SDS/PAGE gel, and the blots were used to detect indicated proteins. Sypro Ruby stain was used on a separate gel to detect a band corresponding to TOR kinases. (*B*) Quantitation of three separate experiments, as in *A*. Asterisk denotes a difference of $P < 0.01$ compared with WT (determined by Student *t*-test).

growth media can also prevent the Fpr1:rapamycin complex from binding to TOR kinases. Farnesol, which leads to superoxide anion production via indirect inhibition of the mitochondrial electron transport chain (27), and hydrogen peroxide, a strong oxidizing agent, can inhibit the binding (Fig. 4*C*). In fact, farnesol can dose-dependently increase the level of superoxide anions without affecting cell proliferation. To determine whether this increase in the level of superoxide anions can lead to a corresponding reduction in rapamycin toxicity, we grew WT cells in the presence of a constant concentration of rapamycin and increasing concentrations of farnesol and measured the doubling time of cells. As expected, farnesol can dose-dependently rescue rapamycin toxicity (Fig. 4*D*).

These findings suggest a universal mechanism for all rapamycin-resistant strains: The elevated levels of superoxide anions prevent

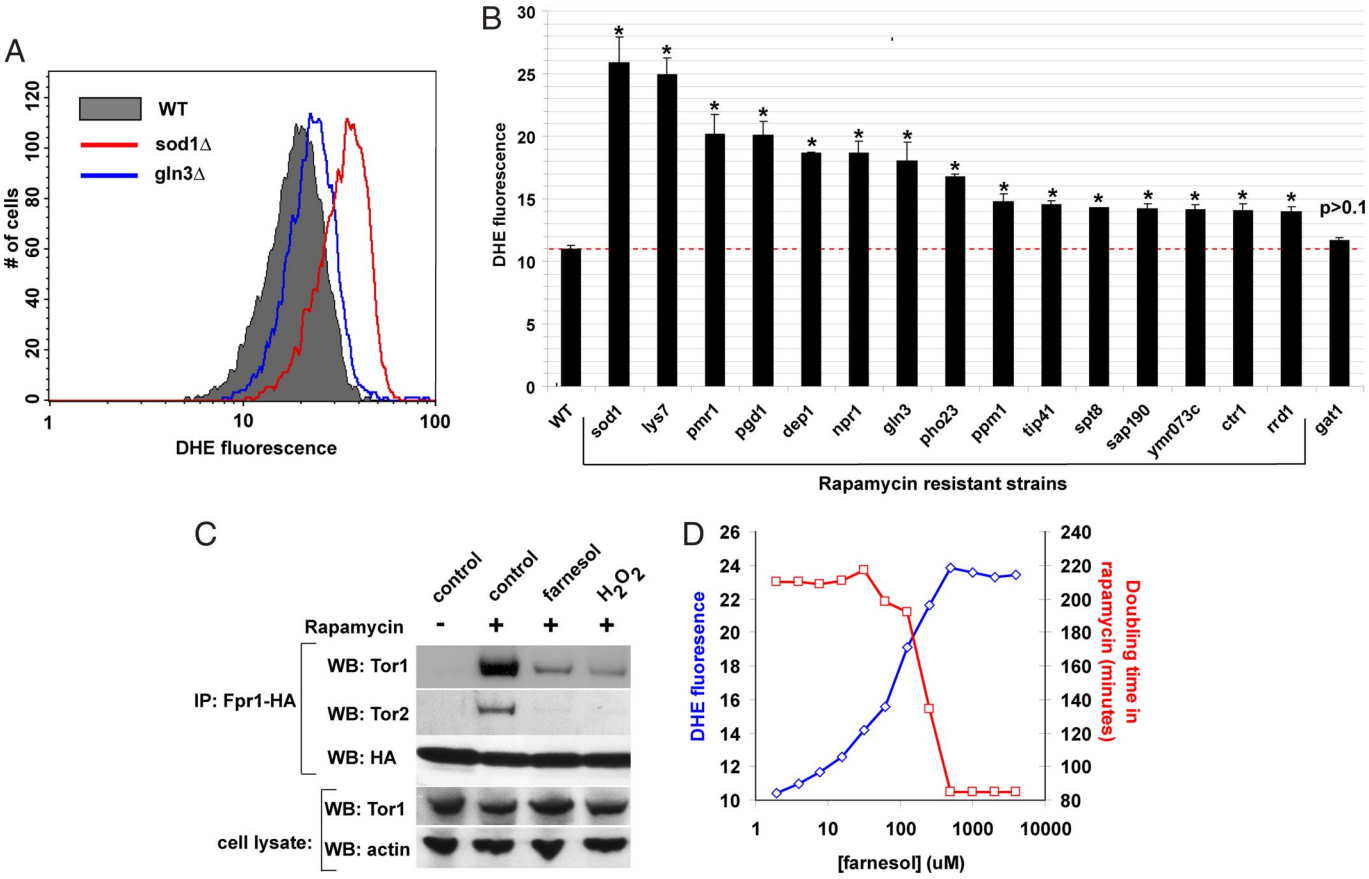

Fig. 4. Oxidative stress by elevated levels of superoxide anions leads to rapamycin resistance. (*A*) Indicated diploid strains growing exponentially were stained with superoxide anion-specific dye DHE in rich YPD media for 1 h. Oxidized version of DHE was detected by flow cytometry. Note the shift in the amount of oxidized DHE in sod1Δ and gln3Δ strains compared with WT cells. (*B*) Quantitative determination of oxidized DHE in all of the rapamycin-resistant strains listed in Table 1. Median autofluorescence (no DHE) was subtracted from the median fluorescence of DHE-treated cells. At least three replicates were performed for each strain. WT and gat1Δ strains served as controls. Asterisk indicates a difference of $P < 0.001$ compared with WT (determined by Student *t*-test). (*C*) WT strain with genomically tagged Fpr1 was grown in the presence of 5 ng/ml rapamycin and either 500 μM farnesol or 2 mM hydrogen peroxide for 2 h. Fpr1 was immunoprecipitated and probed for Tor1 and Tor2. We were unable to determine Tor2 levels in WCL in these experiments. (*D*) Diploid WT cells were grown in the presence of a constant amount of rapamycin (10 ng/ml) and indicated concentrations of farnesol. For each concentration combination, doubling time was determined. A separate aliquot of cells was also stained with DHE, as in *B*.

the formation of the Fpr1:rapamycin:TOR complex. We know from the rapamycin titration profile (Fig. 1*C*) that rapamycin itself does not limit the complex formation, and therefore either Fpr1 or TOR is modified by elevated levels of superoxide anions.

Rapamycin-Resistant Strains Possess Modified TOR Kinase That Prevents Fpr1:Rapamycin Binding. To experimentally determine whether superoxide anions regulate Fpr1 or TOR, we performed two experiments. First, we overexpressed Fpr1 in WT and gln3Δ strains and examined whether this overexpression increases rapamycin sensitivity. If elevated levels of superoxide anions render a fraction of Fpr1 incapable of binding rapamycin and TOR then, presumably, an overexpression of Fpr1 would shift the equilibrium in favor of the Fpr1:rapamycin:TOR complex formation, and hence render cells more rapamycin-sensitive. However, if TOR were modified by superoxide anions in the gln3Δ strain, then overexpression of Fpr1 would have no effect on rapamycin toxicity in gln3Δ strains. Experimentally, we observed the latter case, suggesting that Fpr1 is not limiting and TOR is modified in the rapamycin-resistant cells (Fig. 5*A*). We were unable to perform this experiment with sod1Δ cells, since the overexpression plasmid used a hygromycin B resistance marker, and sod1Δ cells grew very poorly in the presence of both rapamycin and hygromycin B (data not shown).

Second, to verify that TOR kinase is modified in strains with elevated levels of superoxide anions, we performed an *in vitro* lysate binding assay between solid-support attached Fpr1 and TOR kinase from whole-cell lysate (WCL) of either WT, gln3Δ, or sod1Δ cells in the presence of rapamycin. If TOR kinase is modified in gln3Δ and sod1Δ cells, as the Fpr1 overexpression data suggest, then less TOR from the WCL of the two mutants should bind to Fpr1 in the presence of rapamycin than when WCL from WT cells is used. We incubated Fpr1-agarose beads with WCL from WT, gln3Δ, and sod1Δ strains in rapamycin containing lysis buffer. (All three strains were of fpr1Δ background to prevent the endogenous Fpr1 from binding TOR). We then washed away unbound lysate and determined the binding of Tor1 to Fpr1-agarose beads. We were unable to detect bound Tor2, presumably because the antigen affinity of the Tor2 antibody is poor compared with the Tor1 antibody. Tor1 from gln3Δ and sod1Δ cells binds to Fpr1-agarose beads at only ≈62% of WT levels (Fig. 5*B*, compare lane 3 to lanes 5 and 7). The degree of reduced binding in sod1Δ and gln3Δ strains is remarkably similar between the *in vivo* and *in vitro* lysate results. These results show that elevated levels of superoxide anions modify the TOR kinase and that this modification prevents the Fpr1:rapamycin complex from binding and inhibiting TORC1. As a result, these cells exhibit partial rapamycin resistance.

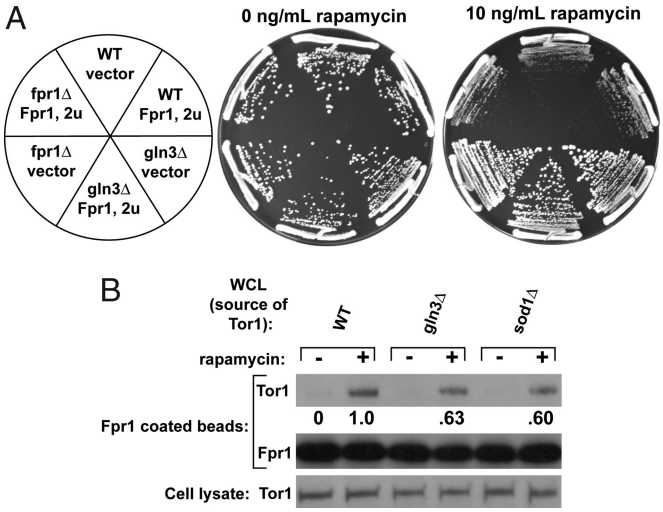

Fig. 5. Elevated levels of superoxide anions modify TOR kinase, not Fpr1. (*A*) Overexpression of Fpr1 does not affect rapamycin resistance of gln3Δ cells. A 2μ-based plasmid expressing Fpr1 was transformed into diploid WT, fpr1Δ, and gln3Δ cells. The same plasmid without Fpr1 served as a control. The cells were plated on YPD plates containing 10 ng/ml rapamycin and hygromycin B for plasmid selection. (*B*) Tor1 kinase from gln3Δ and sod1Δ cells is not fully able to bind to Fpr1-coated beads. Cell extracts from WT, gln3Δ, and sod1Δ cells (all missing endogenous Fpr1) were mixed with Fpr1-coated agarose beads and incubated for 16 h in the presence or absence of rapamycin. The amount of Tor1 bound to agarose beads was determined by washing the beads extensively, resolving the immunoprecipitates by SDS/PAGE, and probing with Tor1 antibody.

Discussion

As the TOR pathway is conserved from yeast to human, we speculated that a dissection of the molecular mechanism of rapamycin resistance in yeast might provide clues to the variation observed in human cancers. Numerous yeast studies have revealed mutants that are rapamycin resistant yet, apart from mutations in Fpr1 and Tor1/2, the molecular reasons for this effect have remained elusive. Our results suggest that care must be exercised when rapamycin is used to inhibit TORC1 in rapamycin-resistant cells, as the resistance might be due to posttranslational modification of TORC1, and full inactivation of TORC1 is not achieved.

TORC1 regulation by oxidative stress has been demonstrated in both yeast and human cells (28–30). Chemically induced oxidative stress leads to activation of TORC1 in mammalian cells, although it is not clear whether this regulation is physiologically relevant. Quantitatively measuring yeast TORC1 activity has remained challenging, as until recently there were no known direct substrates of TORC1. It remains to be determined whether the TORC1 activity is altered in rapamycin-resistant mutants. Also, a previous report has suggested a role for oxidizing environment for intramolecular disulfide bond formation within yeast Tor1, and these disulfide bonds were shown to be responsible for Tor1 stability (30). In our study, we did not observe changes in Tor1 stability in rapamycin-resistant mutants, suggesting a different mechanism for redox regulation of TORC1. Also, rapamycin-resistant sod1Δ and gln3Δ strains did not exhibit altered Kog1 and Lst8 association with TORC1 (data not shown). Further studies must address the mechanism of redox regulation of TORC1 and its role in preventing rapamycin binding to TORC1.

The role of oxidative stress in cancer cells is well established (31), and whether it could serve as a predictor of rapamycin sensitivity in cancer remains to be seen. Reexamination of previous studies using *in vitro* cancer cell lines suggests that rapamycin resistance might arise from the inability of FKBP12:rapamycin to bind mTOR. For instance, rapamycin is much less effective in inhibiting the phosphorylation activity of mTORC1 toward Thr-389 S6K1 in rapamycin-resistant breast cancer cell line MDA-MB-231 than on rapamycin-sensitive cell line MCF7 (8, 10). Direct studies exploring the binding of the FKBP12:rapamycin complex to mTOR and correlating these results with oxidative stress and rapamycin resistance could prove very valuable in defining the clinical uses for rapamycin.

Materials and Methods

Strains, Media, and Reagents. *Saccharomyces cerevisiae* strains used in this study are of S288c background. Sod1 and Gln3 were deleted by homologous recombination from the MAT A hom2Δ deletion strain using hygromycin B marker (hph) from pAG26 (32). Fpr1 was genomically HA tagged using pFA6a-3HA-His3MX6 (33) in indicated haploid MAT A deletion strains. Cells were grown in rich YPD (1% yeast extract, 2% peptone, and 2% glucose) medium at 30°C. Antibodies were obtained from the following sources: Tor1, Tor2, and mouse myc from Santa Cruz Biotechnology; rabbit HA from Bethyl Laboratories; and actin from MP Biomedicals. Rapamycin, farnesol, and hydrogen peroxide were purchased from Sigma.

Deletion Collection Screen. A frozen aliquot of about 20 million cells, made up of 4,757 nonessential diploid knockouts, was allowed to recover in YPD media for

6 h. Rapamycin was added to a final concentration of 7.5 ng/ml, and cells were collected every 12 h. Cultures were kept at logarithmic growth phase. Genomic DNA was isolated by lysis with glass beads followed by phenol/ethanol extraction. The UPTAG and DNTAG molecular bar codes were amplified from ≈0.2 μg of genomic DNA in two separate reactions using biotinylated primers. Amplified UPTAG and DNTAG sequences were combined and used to probe high-density oligonucleotide arrays (Affymetrix Tag3 arrays) at 42°C for 16 h. Washing, staining, and scanning of arrays were performed as previously described (19).

Gene Expression Profile. Rapamycin was added to 150 ml (OD600 = 0.5) of exponentially growing diploid strains to a final concentration of 20 ng/ml for 30 min. Cultures were quickly spun down and cells stored at −80°C until use. mRNA isolation, cDNA synthesis and labeling, and array processing was done as previously described (34).

[^{3}H]Thr Uptake Assay. Exponentially growing diploid cells received either no rapamycin or 5 ng/ml rapamycin in YPD. After 3 h, 0.1 OD600 units of cells (corresponding to ≈2 million cells) was washed with media containing 2% glucose and 0.67% yeast nitrogen base without amino acids. Cells were inoculated in 7.5 ml of this media, and 2.5 μCi of [^{3}H]threonine (Amersham) was added. At indicated time points, 1 ml cells was vacuum filtered onto nitrocellulose filters (Whatman glass microfiber filters, diameter 25 mm) and washed twice with 5 ml PBS. Retained radioactivity was determined by liquid scintillation method. After the last time point, OD_{600} was determined, and it never differed more than 5% between cultures. The blank sample contained 1 ml vacuum-filtered and washed cells without radioactivity.

Cell Lysis, Immunoprecipitation, and Immunoblotting. Exponentially growing cells (OD_{600} = 0.5) were harvested by centrifugation. Cells were washed once with cold PBS and frozen in −80°C until use. A total of 1 ml lysis buffer (PBS, 1 mM EDTA, 1% Nonidet P-40) with protease inhibitors (2 μg/ml aprotinin, 2 μg/ml leupeptin, 1 mM PMSF, 1 mM benzamidine) was used to resuspend the frozen cell pellet. The cell mixture was transferred to a 15-ml Falcon tube containing 400 μl glass beads (500 μm in diameter, Sigma). The tubes were vortexed at 4°C for 10 min. Supernatants were collected after centrifugation at 750 × *g* for 5 min at 4°C, followed by another centrifugation at 10,000 × *g* for 10 min at 4°C. A total of 5 mg total WCL (determined by Bradford assay) in 1 ml was used for immunoprecipitation experiments. A total of 5 μg rabbit HA antibody was added, and immunocomplexes were allowed to form with rotation for 2 h at 4°C. Forty microliters of a 50% slurry of protein A-agarose was then added and incubated another 2 h. Agarose beads were washed with lysis buffer (without protease inhibitors) four times, and the beads were boiled in LDS Sample Buffer (Invitrogen) for 2 min. Immunoprecipitates were resolved by SDS/PAGE, transferred to a nitrocellulose membrane, and probed with indicated antibodies. HRP-labeled secondary antibodies were detected by ECL detection kit (Amersham).

Sypro Ruby Staining. NuPage Bis-Tris gels (Invitrogen) were fixed in 50% methanol, 7% acetic acid for 1 h. The gel was then stained overnight in Sypro Ruby protein gel stain (Molecular Probes). After washing the gel in 10% methanol, 7% acetic acid, the stain was excited at 532-nm wavelength by Typhoon 9400 Imager (Amersham Biosciences). Band intensity quantification was performed with ImageQuant 5.2 (Molecular Dynamics).

Dihydroethidium Staining. Exponentially growing diploid cells were stained with 15 μg/ml of dihydroethidium (DHE) in YPD for 1 h. Cells were washed once in PBS, reinoculated in PBS, and analyzed on a FACSCalibur flow cytometer (Becton Dickinson) through the FL-2 channel. For each strain, median background fluorescence without DHE was subtracted from the intensity of oxidized DHE.

Fpr1 Overexpression. Fpr1 gene was amplified from genomic DNA, along with 600 bp before the start codon and 600 bp after the stop codon. The PCR product was ligated into a multicopy 2μ-based plasmid pRS426 that bears a hygromycin B cassette. The plasmid was transformed into diploid cells, and it was maintained in cells by including 200 μg/ml hygromycin B in the media.

WCL Binding to Fpr1-Coated Beads. Genomically encoded Fpr1-HA was immunoprecipitated from about 10 billion cells using 20 μg anti-HA antibody, as described above. A total of 20 mg WCL from fpr1Δ, fpr1Δsod1, and fpr1Δgln3Δ strains was prepared as described above. Each WCL was split in two: one received no rapamycin and the other received rapamycin at a final concentration of 1 μg/ml. To each WCL tube, an equal amount of Fpr1-coated agarose beads was added. The final incubation volume was 1 ml. The binding was allowed to take place on a rocking platform for 16 h at 4°C. The beads were washed and processed for Western blot analysis as described above.

ACKNOWLEDGMENTS. This work was supported by a National Human Genome Research Institute grant (to R.W.D.).

1. Wullschleger S, Loewith R, Hall MN (2006) TOR signaling in growth and metabolism. *Cell* 124:471–484.
2. Sarbassov DD, Ali SM, Sabatini DM (2005) Growing roles for the mTOR pathway. *Curr Opin Cell Biol* 17:596–603.
3. Sarbassov DD, Guertin DA, Ali SM, Sabatini DM (2005) Phosphorylation and regulation of Akt/PKB by the rictor-mTOR complex. *Science* 307:1098–1101.
4. Kim DH, *et al.* (2002) mTOR interacts with raptor to form a nutrient-sensitive complex that signals to the cell growth machinery. *Cell* 110:163–175.
5. Loewith R, *et al.* (2002) Two TOR complexes, only one of which is rapamycin sensitive, have distinct roles in cell growth control. *Mol Cell* 10:457–468.
6. Sarbassov DD, *et al.* (2004) Rictor, a novel binding partner of mTOR, defines a rapamycin-insensitive and raptor-independent pathway that regulates the cytoskeleton. *Curr Biol* 14:1296–1302.
7. Urban J, *et al.* (2007) Sch9 is a major target of TORC1 in Saccharomyces cerevisiae. *Mol Cell* 26:663–674.
8. Chen Y, Zheng Y, Foster DA (2003) Phospholipase D confers rapamycin resistance in human breast cancer cells. *Oncogene* 22:3937–3942.
9. Neshat MS, *et al.* (2001) Enhanced sensitivity of PTEN-deficient tumors to inhibition of FRAP/mTOR. *Proc Natl Acad Sci USA* 98:10314–10319.
10. Noh WC, *et al.* (2004) Determinants of rapamycin sensitivity in breast cancer cells. *Clin Cancer Res* 10:1013–1023.
11. Hosoi H, *et al.* (1998) Studies on the mechanism of resistance to rapamycin in human cancer cells. *Mol Pharmacol* 54:815–824.
12. Margolin K, *et al.* (2005) CCI-779 in metastatic melanoma: a phase II trial of the California Cancer Consortium. *Cancer* 104:1045–1048.
13. Galanis E, *et al.* (2005) Phase II trial of temsirolimus (CCI-779) in recurrent glioblastoma multiforme: a North Central Cancer Treatment Group Study. *J Clin Oncol* 23:5294–5304.
14. Witzig TE, *et al.* (2005) Phase II trial of single-agent temsirolimus (CCI-779) for relapsed mantle cell lymphoma. *J Clin Oncol* 23:5347–5356.
15. Hudes G, *et al.* (2007) Temsirolimus, interferon alfa, or both for advanced renal-cell carcinoma. *N Engl J Med* 356:2271–2281.
16. Iwenofu OH, *et al.* (2008) Phospho-S6 ribosomal protein: a potential new predictive sarcoma marker for targeted mTOR therapy. *Mod Pathol* 21:231–237.
17. Cloughesy TF, *et al.* (2008) Antitumor activity of rapamycin in a Phase I trial for patients with recurrent PTEN-deficient glioblastoma. *PLoS Med* 5:e8.
18. Tabernero J, *et al.* (2008) Dose- and schedule-dependent inhibition of the mammalian target of rapamycin pathway with everolimus: a phase I tumor pharmacodynamic study in patients with advanced solid tumors. *J Clin Oncol* 26:1603–1610.
19. Giaever G, *et al.* (2002) Functional profiling of the Saccharomyces cerevisiae genome. *Nature* 418:387–391.
20. Xie MW, *et al.* (2005) Insights into TOR function and rapamycin response: chemical genomic profiling by using a high-density cell array method. *Proc Natl Acad Sci USA* 102:7215–7220.
21. Chan TF, Carvalho J, Riles L, Zheng XF (2000) A chemical genomics approach toward understanding the global functions of the target of rapamycin protein (TOR). *Proc Natl Acad Sci USA* 97:13227–13232.
22. Culotta VC, *et al.* (1997) The copper chaperone for superoxide dismutase. *J Biol Chem* 272:23469–23472.
23. Cardenas ME, Cutler NS, Lorenz MC, Di Como CJ, Heitman J (1999) The TOR signaling cascade regulates gene expression in response to nutrients. *Genes Dev* 13:3271–3279.
24. Lorenz MC, Heitman J (1995) TOR mutations confer rapamycin resistance by preventing interaction with FKBP12-rapamycin. *J Biol Chem* 270:27531–27537.
25. Mitchell AP, Magasanik B (1984) Regulation of glutamine-repressible gene products by the GLN3 function in Saccharomyces cerevisiae. *Mol Cell Biol* 4:2758–2766.
26. Bindokas VP, Jordan J, Lee CC, Miller RJ (1996) Superoxide production in rat hippocampal neurons: selective imaging with hydroethidine. *J Neurosci* 16:1324–1336.
27. Machida K, Tanaka T, Fujita K, Taniguchi M (1998) Farnesol-induced generation of reactive oxygen species via indirect inhibition of the mitochondrial electron transport chain in the yeast Saccharomyces cerevisiae. *J Bacteriol* 180:4460–4465.
28. Huang C, *et al.* (2002) Ultraviolet-induced phosphorylation of p70(S6K) at Thr(389) and Thr(421)/Ser(424) involves hydrogen peroxide and mammalian target of rapamycin but not Akt and atypical protein kinase C. *Cancer Res* 62:5689–5697.
29. Sarbassov DD, Sabatini DM (2005) Redox regulation of the nutrient-sensitive raptor-mTOR pathway and complex. *J Biol Chem* 280:39505–39509.
30. Dames SA, Mulet JM, Rathgeb-Szabo K, Hall MN, Grzesiek S (2005) The solution structure of the FATC domain of the protein kinase target of rapamycin suggests a role for redox-dependent structural and cellular stability. *J Biol Chem* 280:20558–20564.
31. Benhar M, Engelberg D, Levitzki A (2002) ROS, stress-activated kinases and stress signaling in cancer. *EMBO Rep* 3:420–425.
32. Goldstein AL, McCusker JH (1999) Three new dominant drug resistance cassettes for gene disruption in Saccharomyces cerevisiae. *Yeast* 15:1541–1553.
33. Longtine MS, *et al.* (1998) Additional modules for versatile and economical PCR-based gene deletion and modification in Saccharomyces cerevisiae. *Yeast* 14:953–961.
34. Williams RM, *et al.* (2002) The Ume6 regulon coordinates metabolic and meiotic gene expression in yeast. *Proc Natl Acad Sci USA* 99:13431–13436.